

Cite as: X. Che *et al.*, *Science*  
10.1126/science.abc17957 (2021).

# Age and composition of young basalts on the Moon, measured from samples returned by Chang'e-5

Xiaochao Che<sup>1</sup>, Alexander Nemchin<sup>2,1\*</sup>, Dunyi Liu<sup>1,3\*</sup>, Tao Long<sup>1</sup>, Chen Wang<sup>1</sup>, Marc D. Norman<sup>4</sup>, Katherine H. Joy<sup>5</sup>, Romain Tartese<sup>5</sup>, James Head<sup>6</sup>, Bradley Jolliff<sup>7</sup>, Joshua F. Snape<sup>5</sup>, Clive R. Neal<sup>8</sup>, Martin J. Whitehouse<sup>9</sup>, Carolyn Crow<sup>10</sup>, Gretchen Benedix<sup>2,11</sup>, Fred Jourdan<sup>2</sup>, Zhiqing Yang<sup>1</sup>, Chun Yang<sup>1</sup>, Jianhui Liu<sup>1</sup>, Shiwen Xie<sup>1</sup>, Zemin Bao<sup>1</sup>, Runlong Fan<sup>1</sup>, Dapeng Li<sup>3</sup>, Zengsheng Li<sup>3</sup>, Stuart G. Webb<sup>8</sup>

<sup>1</sup>Beijing Sensitive High Resolution Ion Micro Probe Center, Institute of Geology, Chinese Academy of Geological Sciences, Beijing 100037, China. <sup>2</sup>School of Earth and Planetary Sciences, Curtin University, Perth, WA 6845, Australia. <sup>3</sup>Shandong Institute of Geological Sciences, Jinan, Shandong 250013, China. <sup>4</sup>Research School of Earth Sciences, The Australian National University, Canberra, ACT 2601, Australia. <sup>5</sup>Department of Earth and Environmental Sciences, The University of Manchester, Manchester M13 9PL, UK. <sup>6</sup>Department of Earth, Environmental, and Planetary Sciences, Brown University, Providence, RI 02912, USA. <sup>7</sup>Department of Earth and Planetary Sciences and The McDonnell Center for the Space Sciences, Washington University in St. Louis, St. Louis, MO 63130, USA. <sup>8</sup>Department of Civil and Environmental Engineering and Earth Sciences, University of Notre Dame, Notre Dame, IN 46556, USA. <sup>9</sup>Department of Geosciences, Swedish Museum of Natural History, SE-104 05 Stockholm, Sweden. <sup>10</sup>Department of Geological Sciences, University of Colorado Boulder, Boulder, CO 80309, USA. <sup>11</sup>Planetary Science Institute, Tucson, AZ 85719, USA.

\*Corresponding author: liudunyi@bjshrimp.cn (D.L.); a.nemchin@curtin.edu.au (A.N.)

**Orbital data indicate that the youngest volcanic units on the Moon are basalt lavas in Oceanus Procellarum, a region with high levels of the heat-producing elements potassium, thorium, and uranium. The Chang'e-5 mission collected samples of these young lunar basalts and returned them to Earth for laboratory analysis. We measure an age of  $1963 \pm 57$  Ma for these lavas and determine their chemical and mineralogical compositions. This age constrains the lunar impact chronology of the inner Solar System and the thermal evolution of the Moon. There is no evidence for high concentrations of heat-producing elements in the deep mantle of the Moon that generated these lavas, so alternate explanations are required for the longevity of lunar magmatism.**

The Oceanus Procellarum region of the Moon is characterized by high concentrations of potassium, thorium, and uranium, elements that generate heat through long-lived radioactive decay and may have sustained prolonged magmatic activity on the near side of the Moon. The Chang'e-5 spacecraft landed in this region at 43.06°N, 51.92°W, about 170 km ENE of Mons Rümker, a location selected as it was expected to host the youngest basalt lavas on the Moon. Orbital data have shown that the geologic unit (designated Em4/P58) exposed around the landing site has high levels of Th (5–8.5 ppm), intermediate to high Ti abundances (5–8% TiO<sub>2</sub>), and high concentrations of the minerals clinopyroxene and olivine (about 31 and 13%, respectively) (1–3). The mission goal was to return samples of young lunar basalts, identified by the spatial density of impact craters (1, 4).

The number of impact craters on a surface reflects its relative age, with older surfaces having more craters. The Moon is the only planetary body where impact crater ages have been calibrated with radiometric dating, so the lunar chronology is used to infer the ages of other planetary surfaces throughout the Solar System. For example, the climatic evolution of Mars is related directly to the lunar cratering chronology. However, the lunar chronology is highly uncertain for ages younger than ~3 Ga (5).

Young volcanism on a small body such as the Moon is

challenging to explain in its thermal evolution. Although the young basaltic eruptions on the Moon occurred in regions of elevated heat-producing elements such as K, Th, and U, it is unclear whether this association is responsible for melting the source magma deep within the Moon (6, 7).

We present mineralogical, chemical and U-Th-Pb isotopic characteristics of two basalt fragments collected by the Chang'e-5 mission. Our goal was to constrain the age of the Em4/P58 basaltic unit at the landing site, which has a wide range of predicted ages based on impact craters, varying from 1.2 to 3.2 Ga (1, 3, 8–14). We also measured the compositions of these basalts to assess their magmatic source and petrogenesis, and to provide calibration for estimates of lunar surface compositions based on remote observations (15).

We analyzed two fragments from the Chang'e-5 samples, which we refer to as CE5-B1 and CE5-B2 (16). Both are equidimensional, approximately 3–4 mm in size and consist of minerals common in lunar basalts, such as chemically zoned clinopyroxene, plagioclase, olivine, and ilmenite, with small amounts of quartz and cristobalite (Fig. 1, data S1, and supplementary text). Both contain multiple interstitial pockets of K-rich glass, barium K-feldspar, troilite, Ca-phosphates (apatite and merrillite), and the Zr-rich minerals baddeleyite and zirconolite. Metallic iron is absent. Both fragments have igneous textures that differ slightly in grain size and crystal

habits: CE5-B1 is finer-grained ( $\leq 1$  mm long) with radiating elongated crystals of plagioclase and ilmenite, whereas CE5-B2 is coarser-grained ( $< 2$  mm long) (Fig. 1 and supplementary text). These textures indicate crystallization from a molten magma (melt) and that CE5-B1 cooled more rapidly than CE5-B2. Most mineral phases in CE5-B2 are highly fractured, and shock-melt pockets and veins (a few tens of microns wide) are present along one edge of the sample (Fig. 1D). In contrast, CE5-B1 has no obvious shock-melt pockets or veins and displays fewer fractures  $\sim 1$  to 10 microns in width. Raman analysis of major, and some accessory, minerals in both fragments (supplementary text) indicates that shock-induced maskelynite is present only in the shock melt zone of fragment CE5-B2. All other minerals (including plagioclase) outside of this zone have not been modified by shocks and preserve their primary magmatic crystallinity (supplementary text).

The pyroxenes and olivines in the two fragments vary widely in their Mg/Fe ratio and include highly Fe-rich compositions for lunar basalts (data S1). The mineral chemistries of these two fragments differ slightly and appear to correspond to their textures (data S1). For example, the olivine in CE5-B2 is more Fe-rich whereas CE5-B1 has a wider range of TiO<sub>2</sub>, Al<sub>2</sub>O<sub>3</sub>, and Cr<sub>2</sub>O<sub>3</sub> in pyroxene (data S1). The mineralogy of these fragments is similar to that of other known lunar basalts. The K-rich glass and the presence of Zr-bearing minerals raise the possibility of a mantle component enriched in heat-producing elements, but these basalts appear to be compositionally fractionated, so the presence of these evolved minerals may instead reflect a small degree of partial melting and/or extensive fractional crystallization.

The bulk compositions of both fragments calculated from their modal mineralogy indicate elevated FeO ( $\sim 22$ -25 wt.%) and low MgO ( $\sim 5$  wt.%). Their TiO<sub>2</sub> contents ( $\sim 6$ -8 wt.%) Al<sub>2</sub>O<sub>3</sub>, ( $< 11$  wt.%), and K concentrations ( $< 2000$  ppm) are consistent with high-Ti, low-Al, low-K mare basalts in standard classifications (17) (Fig. 2 and table S1). The mineralogy and bulk compositions of these samples are consistent with remote sensing observations of this region, implying that they are representative samples of the Em4 unit, despite the differences in grain size and inferred cooling history of CE5-B1 and CE5-B2. However, given the small size of these fragments it is possible that these calculated bulk compositions are not fully representative of the melts from which they formed, especially for the coarser-grained fragment CE5-B2.

The Pb isotope ratios of the two fragments were analyzed in 50 selected locations (spots of about 7  $\mu\text{m}$  in diameter) within phosphate grains, barian K-feldspar grains, K-rich glass pockets, and areas containing Zr-rich minerals (Fig. 3 and data S4). Determining U-Th-Pb ages of lunar basalts requires knowledge of their initial Pb composition. We adopt an isochron approach, in which the data are presented in

$^{207}\text{Pb}/^{206}\text{Pb}$  vs.  $^{204}\text{Pb}/^{206}\text{Pb}$  coordinates. This method allows both the age and the initial Pb isotopic composition to be obtained and has previously been demonstrated through the Pb-Pb study of multiple Apollo basalts (16, 18). The ubiquitous presence of terrestrial contamination in all lunar samples complicates interpretation of the data but is also accounted for in the isochron approach. The individual isochron ages obtained for fragments CE5-B1 and CE5-B2 are  $1893 \pm 280$  Ma and  $1966 \pm 59$  Ma, respectively. Combining all data for the two fragments, which are consistent within uncertainties, gives an age of  $1963 \pm 57$  Ma (Fig. 3A). Our estimate of the initial lunar Pb isotopic composition ( $^{204}\text{Pb}/^{206}\text{Pb} = 0.00226 \pm 0.00006$ ,  $^{207}\text{Pb}/^{206}\text{Pb} = 0.815 \pm 0.009$  and  $^{208}\text{Pb}/^{206}\text{Pb} = 0.926 \pm 0.013$ ) is provided by the intercept of the isochron and a linear model fitted to four K-feldspar analyses (Fig. 3A).

Although these basalt fragments could be susceptible to partial resetting of the U-Pb system, during impacts that transported the fragments to the Chang'e-5 landing site or through subsequent Pb contamination from the host soil, we see no compelling evidence of this in the sample. Shock effects are apparent in one part of CE5-B2, but no isotopic analyses were conducted in this part of the fragment (fig. S6). Any secondary processes that mobilized Pb would also cause excess scatter in the isochron (i.e., specific minerals offset from the isochron by more than expected from the analytical uncertainties). Glass is most prone to Pb exchange, whereas Zr-rich minerals are likely to better preserve their original Pb isotope compositions even if shocked (19). Shock-induced scatter would also be indicated by a large decrease of  $^{207}\text{Pb}/^{206}\text{Pb}$  in less resistant phases; instead, we find the opposite trend in the  $^{207}\text{Pb}/^{206}\text{Pb}$  vs.  $^{204}\text{Pb}/^{206}\text{Pb}$  relationships (Fig. 3). The best fitting isochron constrained using only Zr-rich minerals indicates an age of  $2011 \pm 50$  Ma, consistent with the full dataset (Fig. 3B). The spatially limited distribution of shock effects and intensity in different parts of the fragments, combined with the internal Pb isotope systematics of the samples, indicate that our measurements closely reflect the primary magmatic compositions of these samples.

Mineral and chemical characteristics of the two basalt fragments are consistent with those inferred for the Em4 unit identified at the landing site using remote sensing data (1, 2). Our isochron age is, therefore, representative of the emplacement age of Em4/P58 unit and has implications for lunar cratering chronology. Current model ages of the Em4 unit based on crater density measurements range widely from 1.21 Ga (10) to 3.3 Ga (1), with the results of 1.91 Ga [(3), their model A] and 2.07 Ga (13) being closest to our measured Pb-Pb crystallization age of 1.96 to 2.01 Ga. If this age is representative of the Em4 unit, it implies that nearly 2000 km<sup>3</sup> of basaltic magma (1) erupted near the landing site almost 1 billion years later than the emplacement of any previously measured lunar

basalts in the Apollo, Luna, and lunar meteorite sample collections (18).

Chemical compositions of the two fragments are distinct from those of lunar basalts from other landing sites (Fig. 2). The Chang'e-5 basaltic fragments are more enriched in Fe and depleted in Mg than other sampled lunar basalts, which implies either an Fe-rich mantle source or unusual conditions of emplacement that allowed a greater extent of fractional crystallization of the magmas sampled by Chang'e-5. Extreme fractionation of the basaltic magmas may have contributed to the high Th concentrations measured remotely at the landing site (5-9 ppm). Alternatively, the high Th concentrations inferred from the remote sensing data may reflect either impact ejecta from the surrounding Oceanus Procellarum region, or a primary magmatic component in the source of the Em4 basalts that links their petrogenesis to their spatial association with the high-Th region of the Oceanus Procellarum. The contribution of K-U-Th in the magmatic source or as a contaminant introduced during ascent and evolution of the magma can be assessed by the initial Pb isotopic composition, as determined from the Pb-Pb isochrons. Assuming that the Pb-Pb system remained closed after the formation of these basalts and applying a single-stage Pb isotopic evolution model (16), the source of the melt that formed the Chang'e-5 basalt fragments could have attained a Pb composition similar to that measured in the two fragments if the  $^{238}\text{U}/^{204}\text{Pb}$  ratio of this source (referred to as the  $\mu$ -value) was  $665 \pm 3$ . This model does not consider possible fractionation of U and Pb during the earlier Lunar Magma Ocean (LMO) phase. For example, Apollo mare (formed within lunar maria) and KREEP (high potassium, rare earth elements, and phosphorous) basalts have been used to constrain a multi-stage model of lunar Pb isotopic evolution that indicates a major differentiation event at 4.376 Ga (20), possibly reflecting the final stages of LMO crystallization and formation of the source reservoir for KREEP, which is enriched in all heat-producing elements (20). Applying this multiple-stage Pb isotope model to the Em4 basalts yields a slightly higher  $\mu$ -value of  $677 \pm 3$ .

These  $\mu$ -values for the Em4 basalts imply only a modest (<2%) KREEP component either in their mantle sources or introduced by assimilation during magma ascent. This estimate shows that the Em4 basalts differ from the trend in source evolution previously suggested for Apollo samples, which show a progressive enrichment of their source regions in heat-producing elements as the basalts become younger (18). If this enrichment trend extended to the Em4 basalts it would predict  $\mu$ -values > 1000, which are not observed. Instead, the data suggest only a small amount of KREEP, at most, in these young basalts.

The emplacement age of  $1963 \pm 57$  Ma that we infer for the Em4 unit provides a calibration point for the lunar crater

size-frequency distribution (CSFD) chronology curve, which was previously unconstrained between  $\sim 1$  and 3 Ga (Fig. 4) (5, 21). This age for Em4 falls below many existing crater chronology curves, indicating that the impact flux may have been lower than previously estimated at ages between the youngest Apollo-Luna basalts ( $\sim 3.1$  Ga) and that inferred for the Copernicus crater ( $\sim 0.8$  Ga), consistent with some chronology models (22, 23).  $N(1)$ , the number density of 1 km craters, on the Em4 unit ( $1.24 \times 10^{-3}$  to  $1.74 \times 10^{-3}$   $\text{km}^{-2}$ ) is similar to the upper limit measured for the Copernicus crater [(23, 24); Fig. 4], so Copernicus might be older than the  $\sim 0.8$  Ga radiometric age inferred from the glasses sampled by Apollo 12 (25).

Orbital data indicates the youngest basalts on the Moon are expected within the Oceanus Procellarum, a region of the NW near-side characterized by thin crust and high concentrations of heat-producing elements such as K, Th, and U (7). There is a strong spatial correlation between the occurrence of young lunar basalts and the concentrations of heat-producing elements (26) but the geophysical and geochemical basis for this correlation remains unclear. One possibility is that elevated radioactivity within the lunar mantle produced long-lived thermal anomalies that enhance melting and generate young lunar basalts (7). This hypothesis predicts the young basalts carry elevated levels of heat-producing elements, compared to the basalts that occur outside of the region enriched in these elements. Our Pb isotope results suggest that the Em4 unit and the source of its magma had U and Th contents that were similar to those of Apollo and Luna mare basalts, suggesting that the mantle source regions of the Em4 basalts did not have elevated contents of radioactive elements, and that rising magmas were not mixed with KREEP during passage through the crust. Alternative explanations are required for the longevity of lunar magmatism, such as tidal heating or a distinct source mineralogy supporting lower melting temperature of the mantle. This implies that the elevated Th content of the Em4 regolith recorded in remote sensing data could be due to contamination by secondary ejecta from the Th-rich region of Oceanus Procellarum, which occurs beneath and around the young basalt units (1).

## REFERENCES AND NOTES

1. Y. Qian, L. Xiao, Q. Wang, J. W. Head, R. Yang, Y. Kang, C. H. van der Bogert, H. Hiesinger, X. Lai, G. Wang, Y. Pang, N. Zhang, Y. Yuan, Q. He, J. Huang, J. Zhao, J. Wang, S. Zhao, China's Chang'e-5 landing site: Geology, stratigraphy, and provenance of materials. *Earth Planet. Sci. Lett.* **561**, 116855 (2021). doi:10.1016/j.epsl.2021.116855
2. M. Lemelin, P. G. Lucey, K. Miljković, L. R. Gaddis, T. Hare, M. Ohtake, The compositions of the lunar crust and upper mantle: Spectral analysis of the inner rings of lunar impact basins. *Planet. Space Sci.* **165**, 230–243 (2019). doi:10.1016/j.pss.2018.10.003
3. T. Morota, J. Haruyama, M. Ohtake, T. Matsunaga, C. Honda, Y. Yokota, J. Kimura, Y. Ogawa, N. Hirata, H. Demura, A. Iwasaki, T. Sugihara, K. Saiki, R. Nakamura, S. Kobayashi, Y. Ishihara, H. Takeda, H. Hiesinger, Timing and characteristics of the latest mare eruption on the Moon. *Earth Planet. Sci. Lett.* **302**, 255–266 (2011). doi:10.1016/j.epsl.2010.12.028

4. H. Hiesinger, J. W. Head III, U. Wolf, R. Jaumann, G. Neukum, Ages and stratigraphy of mare basalts in Oceanus Procellarum, Mare Nubium, Mare Cognitum, and Mare Insularum. *J. Geophys. Res.* **108**, 5065 (2003). [doi:10.1029/2002JE001985](https://doi.org/10.1029/2002JE001985)
5. S. J. Robbins, New crater calibrations for the lunar crater-age chronology. *Earth Planet. Sci. Lett.* **403**, 188–198 (2014). [doi:10.1016/j.epsl.2014.06.038](https://doi.org/10.1016/j.epsl.2014.06.038)
6. G. A. Snyder, L. E. Borg, L. E. Nyquist, L. A. Taylor, “Chronology and isotopic constraints on lunar evolution” in *Origin of the Earth and Moon*, R. M. Canup, K. Righter K, Dds. (Univ. Arizona Press, 2000), pp. 361–395.
7. M. Laneuville, J. Taylor, M. A. Wieczorek, Distribution of radioactive heat sources and thermal history of the Moon. *J. Geophys. Res.* **123**, 3144–3166 (2018). [doi:10.1029/2018JE005742](https://doi.org/10.1029/2018JE005742)
8. J. M. Boyce, “Ages of flow units in the lunar nearside maria based on Lunar Orbiter IV photographs” in *Proceedings of the Seventh Lunar Science Conference* (Pergamon Press, 1976), pp. 2717–2728.
9. H. Hiesinger, J. W. Head III, U. Wolf, R. Jaumann, G. Neukum, “Ages and stratigraphy of lunar mare basalts: A synthesis” in *Recent Advances and Current Research Issues in Lunar Stratigraphy*, W. A. Ambrose, D. A. Williams, Eds. (Special Paper 477, Geological Society of America, 2011), pp. 1–51.
10. Y. Q. Qian, L. Xiao, S. Y. Zhao, J. N. Zhao, J. Huang, J. Flahaut, M. Martinot, J. W. Head, H. Hiesinger, G. X. Wang, Geology and scientific significance of the Rümker region in northern Oceanus Procellarum: China’s Chang’E-5 landing region. *J. Geophys. Res.* **123**, 1407–1430 (2018). [doi:10.1029/2018JE005595](https://doi.org/10.1029/2018JE005595)
11. Y. Qian, L. Xiao, S. Yin, M. Zhang, S. Zhao, Y. Pang, J. Wang, G. Wang, J. W. Head, The regolith properties of the Chang’e-5 landing region and the ground drilling experiments using lunar regolith simulants. *Icarus* **337**, 113508 (2020). [doi:10.1016/j.icarus.2019.113508](https://doi.org/10.1016/j.icarus.2019.113508)
12. B. Wu, J. Huang, Y. Li, Y. Wang, J. Peng, Rock abundance and crater density in the candidate Chang’E-5 landing region on the Moon. *J. Geophys. Res.* **123**, 3256–3272 (2018). [doi:10.1029/2018JE005820](https://doi.org/10.1029/2018JE005820)
13. M. Jia, Z. Yue, K. Di, B. Liu, J. Liu, G. Michael, A catalogue of impact craters larger than 200 m and surface age analysis in the Chang’e-5 landing area. *Earth Planet. Sci. Lett.* **541**, 116272 (2020). [doi:10.1016/j.epsl.2020.116272](https://doi.org/10.1016/j.epsl.2020.116272)
14. Y. Qian, L. Xiao, J. W. Head, C. H. van der Bogert, H. Hiesinger, L. Wilson, Young lunar mare basalts in the Chang’e 5 sample return region, northern Oceanus Procellarum. *Earth Planet. Sci. Lett.* **555**, 116702 (2021). [doi:10.1016/j.epsl.2020.116702](https://doi.org/10.1016/j.epsl.2020.116702)
15. D. T. Blewett, P. G. Lucey, B. R. Hawke, B. L. Jolliff, Clementine images of the lunar sample-return stations: Refinement of FeO and TiO<sub>2</sub> mapping techniques. *J. Geophys. Res.* **102**, 16319–16325 (1997). [doi:10.1029/97JE01505](https://doi.org/10.1029/97JE01505)
16. Materials and methods are available as supplementary materials.
17. C. R. Neal, L. A. Taylor, Petrogenesis of mare basalts: A record of lunar volcanism. *Geochim. Cosmochim. Acta* **56**, 2177–2211 (1992). [doi:10.1016/0016-7037\(92\)90184-K](https://doi.org/10.1016/0016-7037(92)90184-K)
18. J. F. Snape, A. A. Nemchin, M. J. Whitehouse, R. E. Merle, T. Hopkinson, M. Anand, The timing of basaltic magmatism at the Apollo landing sites. *Geochim. Cosmochim. Acta* **266**, 29–53 (2019). [doi:10.1016/j.gca.2019.07.042](https://doi.org/10.1016/j.gca.2019.07.042)
19. D. E. Moser, K. R. Chamberlain, K. T. Tait, A. K. Schmitt, J. R. Darling, I. R. Barker, B. C. Hyde, Solving the Martian meteorite age conundrum using micro-baddeleyite and launch-generated zircon. *Nature* **499**, 454–457 (2013). [doi:10.1038/nature12341](https://doi.org/10.1038/nature12341) [Medline](https://www.nature.com/articles/nature12341)
20. L. E. Borg, A. M. Gaffney, C. K. Shearer, A review of lunar chronology revealing a preponderance of 4.34–4.37 Ga ages. *Meteoritics* **50**, 715–732 (2015). [doi:10.1111/maps.12373](https://doi.org/10.1111/maps.12373)
21. D. S. Draper, S. J. Lawrence, R. S. Klima, B. W. Denevi, C. H. van der Bogert, S. M. Elardo, H. H. Hiesinger, The Inner Solar System Chronology (ISOCHRON) lunar sample return mission concept: Revealing two billion years of history. *Planet. Sci. J.* **2**, 79 (2021). [doi:10.3847/PSJ/abe419](https://doi.org/10.3847/PSJ/abe419)
22. W. K. Hartmann, C. Quantin, N. Mangold, Possible long-term decline in impact rates: 2. Lunar impact-melt data regarding impact history. *Icarus* **186**, 11–23 (2007). [doi:10.1016/j.icarus.2006.09.009](https://doi.org/10.1016/j.icarus.2006.09.009)
23. G. Neukum, B. A. Ivanov, W. K. Hartmann, Cratering records in the inner solar system in relation to the lunar reference system. *Space Sci. Rev.* **96**, 55–86 (2001). [doi:10.1023/A:1011989004263](https://doi.org/10.1023/A:1011989004263)
24. H. Hiesinger, C. H. van der Bogert, J. H. Pasckert, L. Funcke, L. Giacomini, L. R. Ostrach, M. S. Robinson, How old are young lunar craters? *J. Geophys. Res.* **117**, E00H10 (2012). [doi:10.1029/2011JE003935](https://doi.org/10.1029/2011JE003935)
25. D. Stöffler, G. Ryder, B. A. Ivanov, N. A. Artemieva, M. J. Cintala, R. A. F. Grieve, Cratering history and lunar chronology. *Rev. Mineral. Geochem.* **60**, 519–596 (2006). [doi:10.2138/rmg.2006.60.05](https://doi.org/10.2138/rmg.2006.60.05)
26. B. L. Jolliff, J. J. Gillis, L. A. Haskin, R. L. Korotev, M. A. Wieczorek, Major lunar crustal terranes: Surface expressions and crust-mantle origins. *J. Geophys. Res.* **105**, 4197–4216 (2000). [doi:10.1029/1999JE001103](https://doi.org/10.1029/1999JE001103)
27. S. Marchi, S. Mottola, G. Cremonese, M. Massironi, E. Martellato, E., A new chronology for the Moon and Mercury. *Astron. J.* **137**, 4936–4948 (2009). [doi:10.1088/0004-6256/137/6/4936](https://doi.org/10.1088/0004-6256/137/6/4936)
28. China National Space Administration, Notice of China National Space Administration on the distribution of procedures for requesting lunar samples (in Chinese and English), 17 December 2020; [www.cnsa.gov.cn/n6758823/n6758839/c6811124/content.html](http://www.cnsa.gov.cn/n6758823/n6758839/c6811124/content.html).
29. J. D. Woodhead, J. M. Hergt, Pb-isotope analyses of USGS reference materials. *Geostand. Geoanal. Res.* **24**, 33–38 (2000). [doi:10.1111/j.1751-908X.2000.tb00584.x](https://doi.org/10.1111/j.1751-908X.2000.tb00584.x)
30. N. Shimizu, S. R. Hart, Applications of the ion microprobe to geochemistry and cosmochemistry. *Annu. Rev. Earth Planet. Sci.* **10**, 483–526 (1982). [doi:10.1146/annurev.ea.10.050182.002411](https://doi.org/10.1146/annurev.ea.10.050182.002411)
31. K. R. Ludwig, *User’s Manual for Isoplot 3.60, A Geochronological Toolkit for Microsoft Excel* (Berkeley Geochronology Center Special Publication No. 4, Berkeley Geochronological Center, 2008).
32. K. P. Jochum, M. Willbold, I. Raczek, B. Stoll, K. Herwig, Chemical Characterisation of the USGS Reference Glasses GSA-1G, GSC-1G, GSD-1G, GSE-1G, BCR-2G, BHVO-2G and BIR-1G Using EPMA, ID-TIMS, ID-ICP-MS and LA-ICP-MS. *Geostand. Geoanal. Res.* **29**, 285–302 (2005). [doi:10.1111/j.1751-908X.2005.tb00901.x](https://doi.org/10.1111/j.1751-908X.2005.tb00901.x)
33. M. Elburg, P. Vroon, B. van der Wagt, A. Tchalian, Sr and Pb isotopic composition of five USGS glasses (BHVO-2G, BIR-1G, BCR-2G, TB-1G, NKT-1G). *Chem. Geol.* **223**, 196–207 (2005). [doi:10.1016/j.chemgeo.2005.07.001](https://doi.org/10.1016/j.chemgeo.2005.07.001)
34. C. Göpel, G. Manhès, C. J. Allegre, U-Pb systematics in iron meteorites—Uniformity of primordial lead. *Geochim. Cosmochim. Acta* **49**, 1681–1695 (1985). [doi:10.1016/0016-7037\(85\)90139-5](https://doi.org/10.1016/0016-7037(85)90139-5)
35. J. Fritz, A. Greshake, D. Stöffler, Micro-Raman spectroscopy of plagioclase and maskelynite in Martian meteorites: Evidence of progressive shock metamorphism. *Antarct. Meteor. Res.* **18**, 96–116 (2005).
36. D. Stöffler, C. Hamann, K. Metzler, Shock metamorphism of planetary silicate rocks and sediments: Proposal for an updated classification system. *Meteorit. Planet. Sci.* **53**, 5–49 (2018). [doi:10.1111/maps.12912](https://doi.org/10.1111/maps.12912)
37. J. J. Papike, F. N. Hodges, A. E. Bence, M. Cameron, J. M. Rhodes, Mare basalts: Crystal chemistry, mineralogy and petrology. *Rev. Geophys. Space Phys.* **14**, 475–540 (1976). [doi:10.1029/RG014i004p00475](https://doi.org/10.1029/RG014i004p00475)
38. J. J. Papike, G. Ryder, C. K. Shearer, Lunar samples. *Rev. Mineral. Geochem.* **36**, 5-01–5-234 (1998).
39. T. L. Grove, D. T. Vaniman, “Experimental petrology of very low Ti/VLT/basalts” in *Mare Crisium: The View from Luna 24*, R. B. Merrill, J. J. Papike, Eds. (Pergamon Press, 1978), pp. 445–471.
40. G. J. Taylor, L. M. V. Martel, P. D. Spudis, The Hadley-Apeninne KREEP basalt igneous province. *Meteorit. Planet. Sci.* **47**, 861–879 (2012). [doi:10.1111/j.1945-5100.2012.01364.x](https://doi.org/10.1111/j.1945-5100.2012.01364.x)
41. MoonDB Search; <http://search.moondb.org/>.
42. T. J. Fagan, D. Kashima, Y. Wakabayashi, A. Sugihara, Case study of magmatic differentiation trends on the Moon based on lunar meteorite Northwest Africa 773 and comparison with Apollo 15 quartz monzodiorite. *Geochim. Cosmochim. Acta* **133**, 97–127 (2014). [doi:10.1016/j.gca.2014.02.025](https://doi.org/10.1016/j.gca.2014.02.025)
43. M. A. Wieczorek, B. L. Jolliff, A. Khan, M. E. Pritchard, B. P. Weiss, J. G. Williams, L. Hood, K. Righter, C. R. Neal, C. K. Shearer, I. S. McCallum, S. Tompkins, B. R. Hawke, C. Peterson, J. J. Gillis, B. Bussey, The constitution and structure of the lunar interior. *Rev. Mineral. Geochem.* **60**, 221–364 (2006). [doi:10.2138/rmg.2006.60.3](https://doi.org/10.2138/rmg.2006.60.3)
44. L. J. Hallis, M. Anand, S. Strekopytov, Trace-element modelling of mare basalt parental melts: Implications for a heterogeneous lunar mantle. *Geochim. Cosmochim. Acta* **134**, 289–316 (2014). [doi:10.1016/j.gca.2014.01.012](https://doi.org/10.1016/j.gca.2014.01.012)

## ACKNOWLEDGMENTS

We thank CNSA for providing access to the Lunar Sample CE5C0000YJYX03501GP.

We also thank Jeff Taylor, Desmond Moser and an anonymous reviewer for their thoughtful reviews that helped to improve our manuscript and Keith Smith for giving us editorial guidance and numerous editorial comments. **Funding:** China National Space Administration (CNSA) Grant Nos. D020204, D020206, D020203 (DL, XCh, TL, ChW). The National Key R & D Program of China from Ministry of Science and Technology of the People's Republic of China Grant No. 2020YFE0202100 (DL, XCh, TL, ChW). Science and Technology Facilities Council ST/R000751/1 and ST/P005225/1 (KHJ, RT). The Royal Society URF\R\201009 (KHJ). The Leverhulme Trust RPG-2019-222 (KHJ). **Author contributions:** XCh, AN, DL, MDN, BJ, KHJ, RT, JFS, JH, CRN designed the project. All authors contributed to the lunar sample request application to CNSA. XCh, AN, DL, TL, ChW, MDN, BJ, KHJ, RT, JFS, MJW, ZhY, ChY, JL, ShX, ZB, RF, DL, ZL collected analytical data. XCh, AN, DL, BJ, KHJ, RT, JFS, CRN, SGW produced tables, figures and performed calculations. AN, MDN, KHJ, RT, JH, JFS, BJ, CRN wrote the draft manuscript. All authors reviewed and edited the manuscript. **Competing interests:** We declare no competing interests. **Data and materials availability:** The lunar sample, designation CE5C0000YJYX03501GP, was provided by the China National Space Administration (CNSA) under a materials transfer agreement (28). The two basalt fragments CE5-B1 and CE5-B2 are currently held at the Beijing Sensitive High Resolution Ion Micro Probe Center on a one-year loan (with a possible extension for another year), after which they will be returned to CNSA. Readers may request Chang'e-5 samples from CNSA through a standard procedure (28). Further details are provided in the supplementary materials. Our EMP data are provided in data S1 to S3, the Pb isotope results in data S4, and the Raman measurements in data S5 and S6. Calculated bulk compositions of two fragments are given in table S1.

## SUPPLEMENTARY MATERIALS

[science.org/doi/10.1126/science.abl7957](https://doi.org/10.1126/science.abl7957)

Materials and Methods

Supplementary Text

Figs. S1 to S13

Table S1

References (29–44)

Data S1 to S6

5 August 2021; accepted 23 September 2021

Published online 7 October 2021

10.1126/science.abl7957

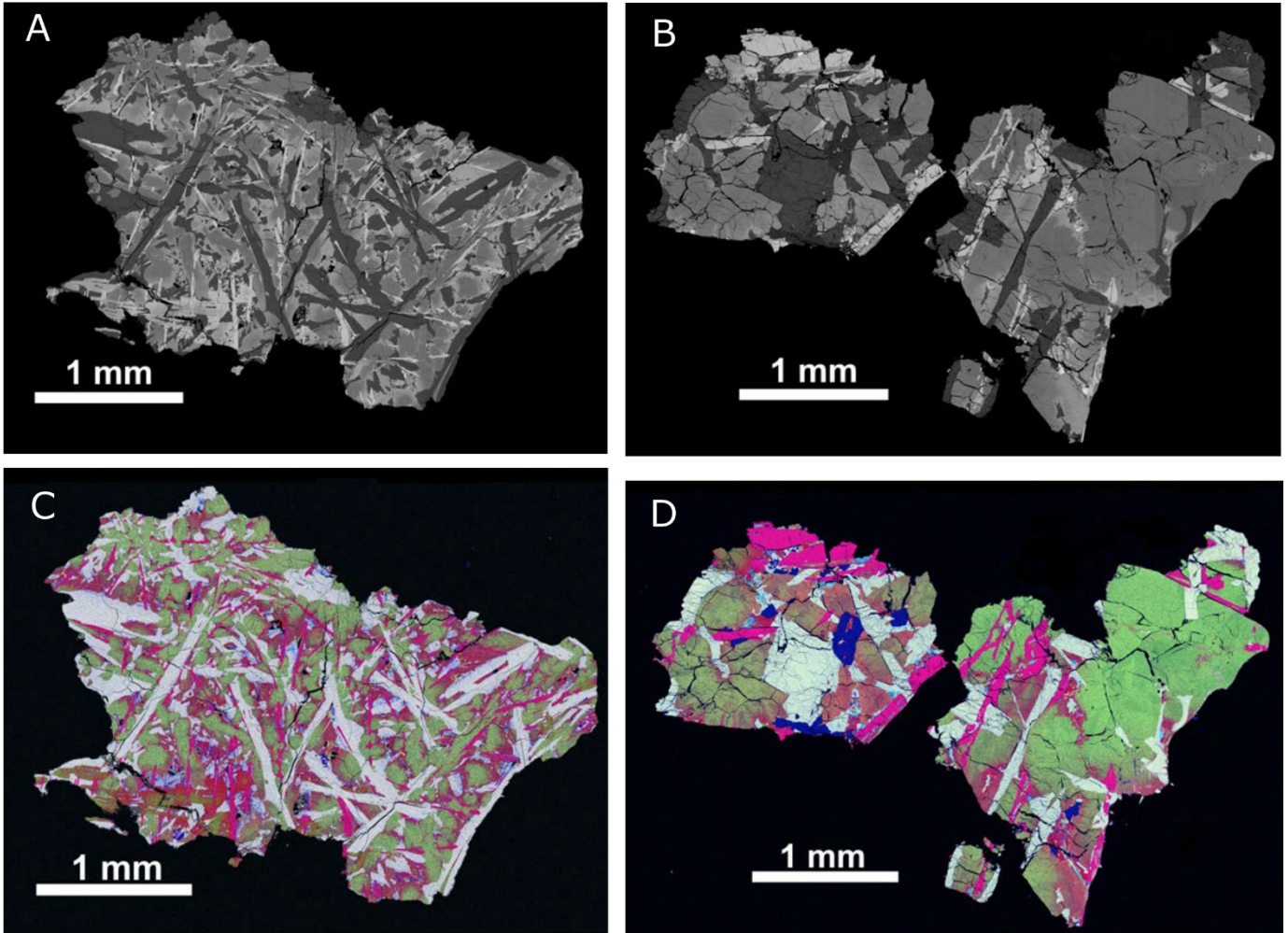
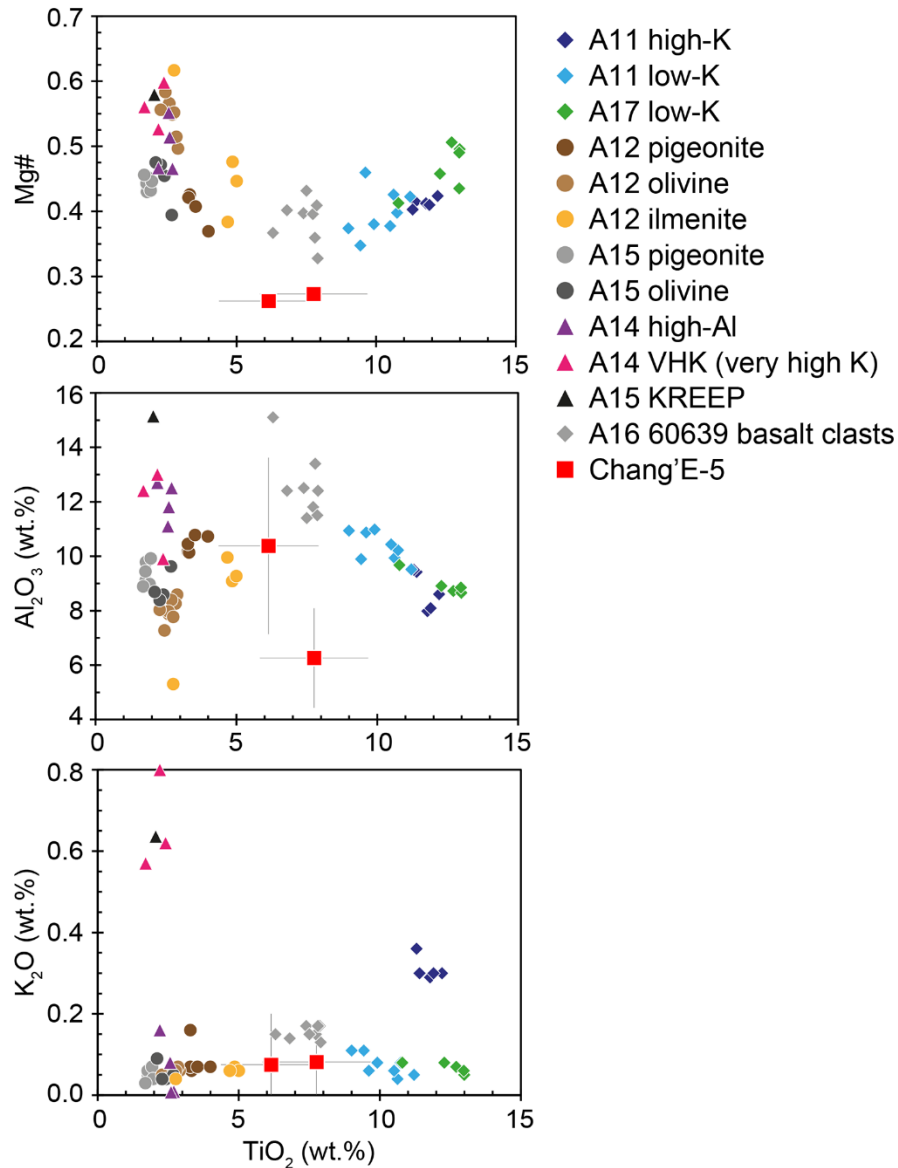
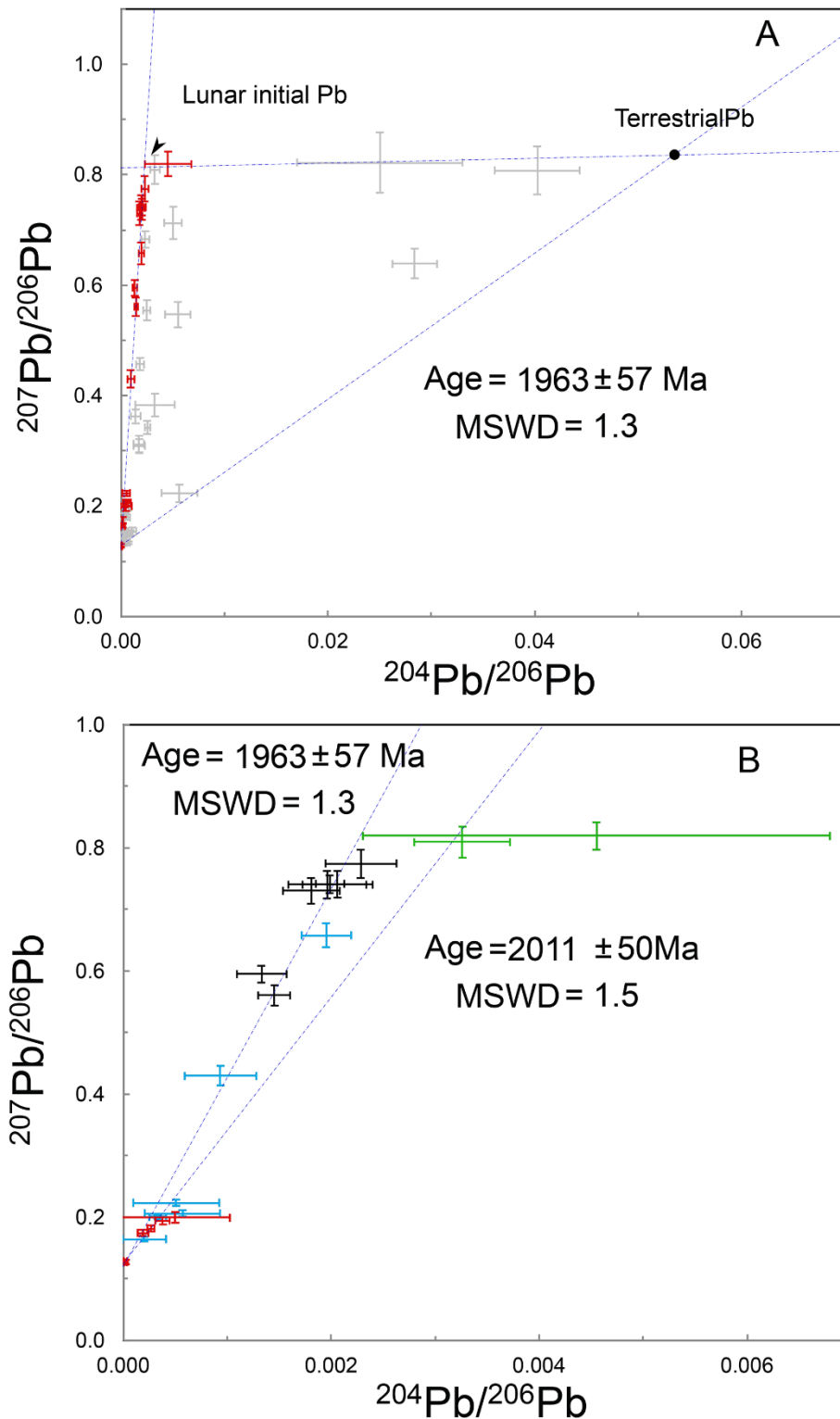


Fig. 1. Back-scattered electron (BSE) images and false color energy dispersive spectroscopy (EDS) element maps of the two fragments from the Chang'e 5 sample. (A and B) BSE images of CE-5-B1 and CE-5-B2, respectively. (C and D) EDS images of CE-5-B1 and CE-5-B2. Qualitative concentration and distribution of different elements in both samples are represented by different colors: blue=silica, green=Mg, red=Fe, white=Al, yellow=Ca, pink=Ti, cyan=K.



**Fig. 2. Bulk chemical composition of basalt fragments.** Mg# [defined as  $Mg/(Mg+Fe)$ ],  $Al_2O_3$  and  $K_2O$  vs.  $TiO_2$  measurements for the two analyzed Chang'e-5 fragments (red squares with 1 sigma error bars). These are compared to different basalts from Apollo landing sites as indicated in the legend (A11 stands for Apollo 11 etc. A16 60639 refers to Apollo 16 sample 60639).



**Fig. 3. Pb-Pb isotope data and isochrons for CE-5-B1 and CE-5-B2.** (A) Data for all measured points in the sample. Red points indicate analyses used to define the isochron, while grey points are analyses affected by terrestrial contamination. Black dot shows terrestrial Pb composition representing contamination. Blue dashed lines define mixing triangle (16), where steep line at the left is the isochron defining the age of the sample, line at the top is the best fit of four K-feldspar analyses used to determine initial Pb composition, line at the bottom is mixing line with terrestrial Pb. MSWD is mean squared weighted deviation. (B) Analyses used to define the isochron: red data points are Zr minerals, light blue are phosphates, green are K-feldspar, black are K-glass. The blue lines show isochron constrained from all minerals [as in (A)] and the best fit line defined by analyses of Zr-rich minerals. All error crosses are at 2 sigma.

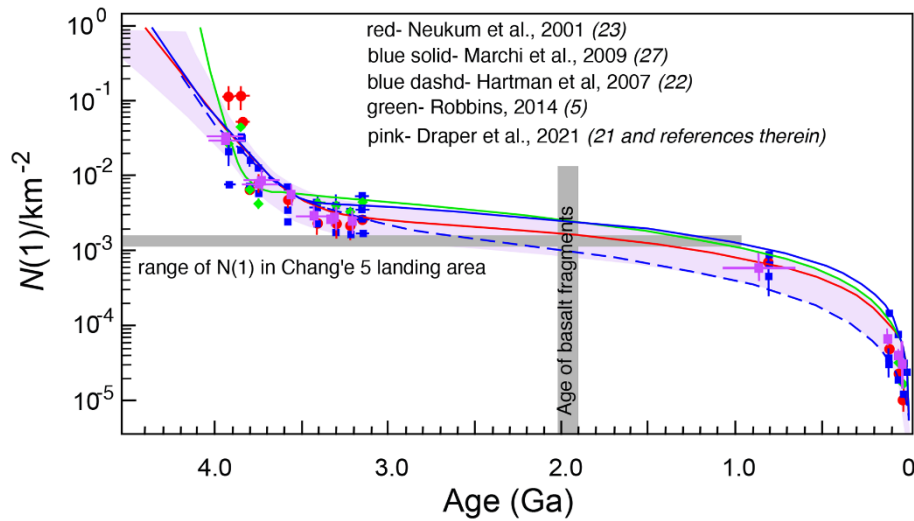


**Fig. 4. Lunar cratering chronology models compared to our measurement of the Chang'e-5 sample.** Each model relates the radiometric and exposure ages of lunar samples to the frequency of 1-km impact craters  $N(1)$  on each sampled unit. The grey shaded areas indicate the age of Chang'e-5 basalt fragments (this study) and the range of  $N(1)$  estimates for the site (1, 3, 12, 13). Data used to constrain the curves are from (5, 21–23, 27).

## Age and composition of young basalts on the Moon, measured from samples returned by Chang'e-5

Xiaochao Che, Alexander Nemchin, Dunyi Liu, Tao Long, Chen Wang, Marc D. Norman, Katherine H. Joy, Romain Tartese, James Head, Bradley Jolliff, Joshua F. Snape, Clive R. Neal, Martin J. Whitehouse, Carolyn Crow, Gretchen Benedix, Fred Jourdan, Zhiqing Yang, Chun Yang, Jianhui Liu, Shiwen Xie, Zemin Bao, Runlong Fan, Dapeng Li, Zengsheng Li, and Stuart G. Webb

*Science*, Ahead of Print

### View the article online

<https://www.science.org/doi/10.1126/science.abl7957>

### Permissions

<https://www.science.org/help/reprints-and-permissions>